Details of the cross-validation for the order

We estimate of the order of each time series according to the order-consistent, nonparamteric method of Tong and co-workers [1,2] – see 'testing the method' (below) for a study of the power of the method when used on ecological data. Since there is fairly strong correlation between adjacent observations, we removed 7 observations prior to estimating the locally-linear regression against lagged-abundances. In this way and spurious pattern resulting from strong serial correlation is avoided [3] (Box 1 in main text). In the text we estimate the order by summarising the evidence across the replicates (Fig. 2). In this supplement we break the results down by replicates. The results are highly consistent across replicates. D_{opt} in the table below is the estimated order. CV represents the cross-validation error. D_{2nd} represents the second best estimate. The last five columns show the entire cross-validation profiles for each replicate (h is the bandwidth of the Gaussian kernel). The bandwidth is also optimised using cross-validation. The order that is predicted by the model (see Table 2) is highlighted in boldface.

Rep.	Sp.	N	D_{opt}(CV)	D_{2nd}(CV)	D=1 (h)	D=2 (h)	D=3 (h)	D=4 (h)	D=5 (h)
PV1	*P.i.*	130	4 (0.36)	**5 (0.37)**	0.63 (1.5)	0.38 (0.5)	0.46 (1.5)	0.36 (1.1)	0.37 (1.5)
PV1	*P.i.*	127	**5 (0.62)**	4 (0.66)	0.71 (3.0)	0.68 (3.0)	0.67 (1.5)	0.66 (1.6)	0.62 (10)
PV2	*P.i.*	130	**5 (0.33)**	3 (0.48)	0.67 (0.9)	0.50 (1.2)	0.48 (1.3)	0.50 (1.4)	0.33 (1.5)
PV2	*V.c.*	127	**5 (0.39)**	4 (0.45)	0.54 (10)	0.45 (10)	0.41 (3)	0.40 (1.2)	0.39 (1.4)
PV3	*V.c.*	77	**5 (0.39)**	4 (0.40)	0.55 (10)	0.52 (10)	0.51 (3)	0.45 (1.8)	0.40 (2)
PV3	*V.c.*	74	**5 (0.36)**	4 (0.44)	0.53 (0.6)	0.49 (1.3)	0.47 (10)	0.44 (1)	0.36 (1.3)
PP1	*P.i.*	74	**3 (0.29)**	2 (0.30)	0.64 (0.3)	0.30 (0.8)	0.29 (1)	0.37 (1.3)	0.39 (1.4)
PP2	*P.i.*	88	**3 (0.53)**	4 (0.57)	0.82 (10)	0.57 (1.6)	0.53 (2)	0.57 (3)	0.61 (2)
PP3	*P.i.*	91	2 (0.58)	1 (0.60)	0.60 (1.3)	0.58 (1.4)	0.61 (2)	0.64 (2)	0.64 (2)
P1	*P.i.*	95	**3 (0.52)**	2 (0.55)	0.72 (0.7)	0.55 (10)	0.52 (4)	0.55 (10)	0.56 (3)
P2	*P.i.*	48	2 (0.36)	**3 (0.38)**	0.75 (10)	0.36 (1.6)	0.38 (1.8)	0.43 (10)	0.48 (10)
P3	*P.i.*	108	5 (0.42)	**3 (0.46)**	0.80 (0.6)	0.50 (0.6)	0.46 (0.9)	0.49 (1.3)	0.42 (1.4)

Testing the power of the order estimation

In the main text we reported a subset of our analysis of the power of the order-consistent nonparametric method when applied to time series from three well-known age-/stage- structured models. In each instance we simulated the models for 150 time-steps, and discarded the first 50 observations. The resulting time series – of comparable length (100 observations) to the replicates analysed above – are subjected to identical analyses to those of the real data. We repeated the simulation and analysis 25 times for each model. The simplest model is a (non-age-structured) one-dimensional stochastic Ricker model [4]. The second model is the three-dimensional LPA-model for the stage-structured dynamics of the flour beetle [5]. The third model is an age-structured model for fish dynamics [6], where the dimension can be anywhere from 2 to 4 depending on the number of age classes. In the following we report the result for a much wider range of parameter values.

The overall conclusions of the simulation are that the nonparametric method can correctly identify the order (of at least up to four) of time series from diverse ecological systems on the basis of 100 observations. The order tend to be biased upwards for highly nonlinear versions of the models. However, the order is at most increased by one, and the fit of the larger model is only very marginally better (by around 1%). We are therefore confident that the differences reported in the main text arise from biological differences and not from statistical artefacts. And s-plus library to carry out the time series analyses is available from the first author (e-mail: bjornsta@nceas.ucsb.edu).

Ricker model

We estimated the order based on time series of length 100 from different realizations of the stochastic Ricker model

$$N_{t+1} = N_t \exp[r*(1-N_t)]u_t,$$

where N is the scaled denisty, r is the growth rate and u is a sequence of log-normal variates with unit mean and a coefficient of variation of 0.1. The growth rate determines the degree of nonlinearity in the dynamics -- as r increases the dynamics go through a cascade from stable through cyclic to chaotic dynamics. Figure S1 shows the CV profiles for 4 different parameter sets (r = 1.5, 2, 2.5 and 3). The parsimonious order is estimated to be one for all but the last parameter-value, for which order two is concluded. (Note, though, that the difference between order two and order one is only 0.8%.)

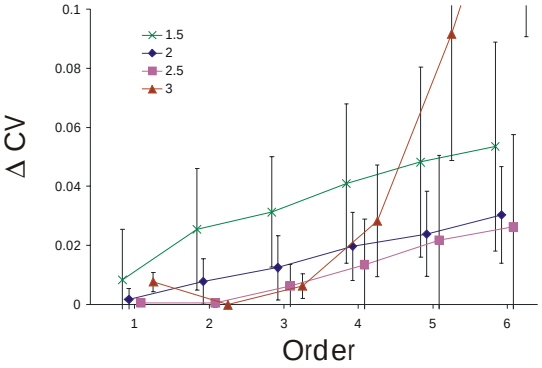

Fig S1: The CV profiles to estimate the order from time series from the Ricker model. The growth rate is varied from 1.5 to 3. The figure reports the results across 25 realisations. Note that the bars represent standard deviations and *not* standard errors of the means. See figure 2in the main text for details.

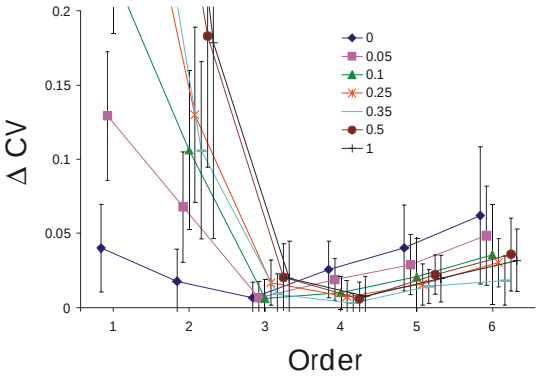

Fig S2: The CV profiles to estimate the order from time series from the three-dimensional LPA model. The growth rate is varied from 1.5 to 3. The figure reports the results across 25 realisations. Note that the bars represent standard deviations and *not* standard errors of the means. See figure 2in the main text for details.

LPA model

We simulated stochastic realizations from the three-dimensional Larvae-Pupae-Adult (LPA) model for the dynamics of *Tribolium* flour beetle populations [5]:

$$L_{t+1} = b\, A_t \exp[-c_{el}\, L_t - c_{ea}\, A_t + E_{1t}]$$
$$P_{t+1} = L_t\,(1 - \mu_l)$$
$$A_{t+1} = P_t \exp[-c_{pa}\, A_t] + A_t\,(1 - \mu_a),$$

where b (= 6.6) represents reproduction; c_{el} (= $1.2*10^{-2}$) andd c_{ea} (=$1.2*10^{-2}$) are cannibalism rates of eggs by pupae and larvae, respectively; μ_l (= 0.2) and μ_a (= 0.8) are larval and adult mortality rates. E_{1t} is a sequence of normal variates with mean zero and variance 0.35. For simplicity we assume reproduction to be the only stochastic event. The parameter values are as given in [5], except for μ_a (which appear to be mistyped in the original paper). The most important control parameter in this model is the adult cannibalism on pupae, c_{pa}. In figure S2 we show the CV profiles for the cannibalism rates studied in [5]: c_{pa} = 0, 0.05, 0.2, 0.25, 0.35, 0.5, and 1. The order is correctly identified as 3 in most cases. However for highly nonlinear processes (large c_{pa}), the order is estimated to be 4. Note, that the difference between order 4 and order 3 is less than 1.5% in these cases.

SR model

We simulate stochastic realisations from the age-structured model of fish dynamics that encompass the interactions between young-of-the-year (X), juveniles (Y), and mature individuals (S) [6]:

$$X_t = b\, S_t\, \alpha_t$$
$$Y_{t+1} = X_t \exp[-\beta \ln(X_t) - \gamma \ln(Y_t)]$$
$$S_{t+1} = (1 - \mu_y)\, Y_t + (1 - \mu_s)\, S_t,$$

where b (= 13) is the reproduction rate, and α is a sequence of log-normal variates (with mean 1 and a coefficient-of-variation 0.3) that represent stochastic reproduction; β and γ are juvenile competition and cannibalism rates; μ_y (=.1) and μ_s are juvenile and mature mortality rates. The dimension of the model depends on the mortality rates of the mature. Functional semelparity (μ_s = 1) results in a two-dimensional model; biparity (mature individuals reproduce for two years before dying) results in a three-dimensional model; triparity results in a four-dimensional model. In the simulation we use β = 0.5 and γ = 0.4 in the semelparous model, and β = 0.3 and γ = 0.7 in the iteroparous models. Figure S3 shows the CV profiles for the three different models. The order is correctly identified as 2, 3, and 4 respectively.

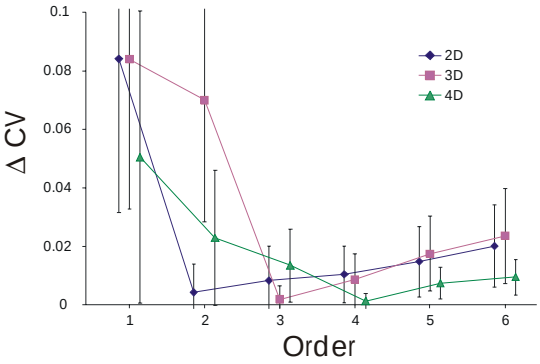

Fig S3: The CV profiles to estimate the order from time series from the 2-, 3-, and 4-dimensional fish model. The figure reports the results across 25 realisations. Note that the bars represent standard deviations and *not* standard errors of the means. See figure 2in the main text for details.

Details pertaining to the delays in regulation

The model (equation 1-2) predicts significant lags in the regulation of *Plodia* (denoted by X) for different experimental treatments (see Table 2). The PP column assumes that the *Plodia*-PiGV interactions does not involve complete coupling (see text):

lag	*Plodia*-*Venturia* (PV)	*Plodia*-PiGV (PP)	*Plodia* (P)
1	X	X	X
3	X	X	X
6	X	X	X
45	X		
78	X		

The observed patterns in the time series -- summarized across the three replicates for each system – are summarized in the table below. '+' denotes a significant positive dependence, '-' denotes a significant negative interaction, and 'ns' denotes no significant interaction:

lag	PV	PP	P	PV: estimates	PP: estimates	P: estimates
1	+	+	+	0.41 (SE = 0.03, p < 0.01)	0.13 (SE = 0.05, p = 0.02)	0.12 (SE = 0.03, p < 0.01)
3	-	-	-	-0.42 (SE = 0.14, p < 0.01)	-0.35 (SE = 0.08, p < 0.01)	-0.12 (SE = 0.04, p < 0.01)
6	+	+	+	0.19 (SE = 0.06, p < 0.01)	0.31 (SE = 0.06, p < 0.01)	0.21 (SE = 0.03, p < 0.01)
45	+	ns	ns	0.18 (SE = 0.05, p < 0.01)	-0.06 (SE = 0.07, p = 0.34)	0.02 (SE = 0.04, p = 0.56)
78	-	ns	ns	-0.52 (SE = 0.12, p < 0.01)	-0.04 (SE = 0.07, p = 0.53)	0.03 (SE = 0.04, p = 0.47)

If we break the analysis into one for each individual replicate, the results are highly consistent in that 41 out of 45 parameter estimates (=5 lags * 3 reps * 3 treatments) show identical signs of dependence to that seen in the across-replicate analysis. The four estimates that break with the predictions are shown in boldface below. Of these, 3 are non-significant. Note though that since the sample size is lower in the individual replicates, the power is lower so that some estimates are no longer statistically significant (denoted by brackets in the tables below).

Plodia-Venturia:
The predicted and observed patterns for each of the three replicates PV1, PV2, and PV3 are summarized in the table. '+' denotes a positive dependence, '-' denotes a negative interaction. Parentheses signify non-significant coefficients.

lag	Pred	PV1	PV2	PV3	PV1: estimates	PV2: estimates	PV3: estimates
1	+	+	+	+	1.12 (SE = 0.09, p < 0.01)	0.65 (SE = 0.09, p < 0.01)	0.82 (SE = 0.2, p < 0.01)
3	-	-	(-)	**0**	-0.31 (SE = 0.1, p < 0.01)	-0.13 (SE = 0.11, p = 0.22)	**0 (SE = 0.18, p = 1)**
6	+	+	+	+	0.34 (SE = 0.14, p = 0.02)	0.59 (SE = 0.11, p < 0.01)	1.07 (SE = 0.18, p < 0.01)
45	+	+	(+)	**(-)**	0.33 (SE = 0.1, p < 0.01)	0.14 (SE = 0.12, p = 0.24)	-0.29 (SE = 0.22, p = 0.19)
78	-	-	-	-	-0.7 (SE = 0.12, p < 0.01)	-0.51 (SE = 0.10, p < 0.01)	**-0.48 (SE = 0.23, p = 0.04)**

Plodia-PiGV:
The predicted and observed patterns for each of the three replicates PP1, PP2, and PP3 are summarized in the table. '+' denotes a positive dependence, '-' denotes a negative interaction. Parentheses signify non-significant coefficients.

lag	Pred	PP1	PP2	PP3	PP1: estimates	PP2: estimates	PP3: estimates
1	+	+	(+)	+	0.19 (SE = 0.12, p = 0.12)	0.07 (SE = 0.12, p = 0.58)	0.48 (SE = 0.1, p < 0.01)
3	-	(-)	-	-	-0.22 (SE = 0.11, p = 0.05)	-0.25 (SE = 0.12, p = 0.04)	-0.44 (SE = 0.09, p < 0.01)
6	+	+	(+)	(+)	0.58 (SE = 0.15, p < 0.01)	0.18 (SE = 0.13, p = 0.15)	0.16 (SE = 0.13, p = 0.2)
45		ns	ns	**+**	-0.18 (SE = 0.14, p = 0.21)	0.12 (SE = 0.13, p = 0.38)	**0.31 (SE = 0.11, p = 0.01)**
78		ns	ns	ns	-0.23 (SE = 0.17, p = 0.18)	0.17 (SE = 0.14, p = 0.25)	-0.05 (SE = 0.12, p = 0.66)

Plodia:
The predicted and observed patterns for each of the three replicates P1, P2, and P3 are summarized in the table. '+' denotes a positive dependence, '-' denotes a negative interaction. Parentheses signify non-significant coefficients.

lag	Pred	P1	P2	P3	P1: estimates	P2: estimates	P3: estimates
1	+	+	(+)	+	0.16 (SE = 0.05, p < 0.01)	0.14 (SE = 0.24, p = 0.56)	0.15 (SE = 0.05, p = 0.01)
3	-	-	(-)	-	-0.11 (SE = 0.05, p = 0.01)	-0.32 (SE = 0.28, p = 0.25)	-0.09 (SE = 0.05, p = 0.06)
6	+	+	**(-)**	+	0.22 (SE = 0.05, p < 0.01)	**-0.08 (SE = 0.24, p = 0.74)**	0.27 (SE = 0.05, p < 0.01)
45		ns	ns	ns	-0.04 (SE = 0.05, p = 0.49)	0.28 (SE = 0.28, p = 0.31)	0.04 (SE = 0.06, p = 0.53)
78		ns	ns	ns	-0.04 (SE = 0.05, p = 0.47)	0.37 (SE = 0.25, p = 0.13)	-0.06 (SE = 0.05, p = 0.27)

Details on the estimation of the 'transmission functions'

We can estimate the functions F, G, H, and K based on each replicate separately. Each function is similar in appearance to those shown in figure 3. That is, F is increasing in both I_{t-3} and S_{t-3}; G is increasing in both I_{t-3} and $L_{3,t-3}$; H is increasing in both V_{t-3} and $L_{3-5,t-3}$; K is decreasing in both $V_{t-2/4}$ and $L_{3,t-3}$. Most of the functions are statistically significant despite the power being lower once the replicates are considered separately. The shape-parameters, κ, of the negative binomial are furthermore comparable between replicates. The detailed results are as follows:

Function F: Replicate 1 $F_{90,4} = 6.6$, $p < 0.001$, $\kappa = 2.41$, SE(κ) = 0.35; Replicate 2 $F_{91,4} = 3.0$, $p = 0.02$, $\kappa = 3.55$, SE(κ) = 0.51; Replicate 3 $F_{89,4} = 1.7$, $p < 0.001$, $\kappa = 4.30$, SE(κ) = 0.66.

Function G: Replicate 1 $F_{92, 4} = 5.8$, $p < 0.001$, $\kappa = 1.45$, $SE(\kappa) = 0.19$; Replicate 2 $F_{93, 4} = 1.9$, $p = 0.12$, $\kappa = 1.68$, $SE(\kappa) = 0.23$; Replicate 3 $F_{91, 4} = 0.83$, $p = 0.51$, $\kappa = 1.46$, $SE(\kappa) = 0.20$.

Function H: Replicate 1 $F_{96, 4} = 10.1$, $p < 0.001$, $\kappa = 0.90$, $SE(\kappa) = 0.12$; Replicate 2 $F_{96, 4} = 7.9$, $p < 0.001$, $\kappa = 0.97$, $SE(\kappa) = 0.13$; Replicate 3 $F_{51, 4} = 1.74$, $p = 0.15$, $\kappa = 0.58$, $SE(\kappa) = 0.11$.

Function K: Replicate 1 $F_{96, 4} = 4.6$, $p = 0.002$, $\kappa = 0.56$, $SE(\kappa) = 0.09$; Replicate 2 $F_{96, 4} = 1.9$, $p = 0.11$, $\kappa = 0.78$, $SE(\kappa) = 0.13$; Replicate 3 $F_{51, 4} = 3.66$, $p = 0.01$, $\kappa = 0.69$, $SE(\kappa) = 0.18$.

References

1. Cheng, B. & Tong, H. On consistent nonparametric order determination and chaos. *J. R. Statist. Soc. B* **54**, 427-449 (1992).
2. Yao, Q. & Tong, H. Quantifying the influence of initial values on non-linear prediction. *J. R. Statist. Soc. B* **56**, 701-725 (1994).
3. Ellner, S. & Turchin, P. Chaos in a noisy world: New methods and evidence from time-series analysis. *Am. Nat.* **145**, 343-375 (1995).
4. Ricker, W.E. Stock and recruitment. *Journal of Fishery Research Board Canada* **11**, 559-623 (1954).
5. Costantino, R.F., Desharnais, R.A., Cushing, J.M. & Dennis, B. Chaotic dynamics in an insect population. *Science* **275**, 389-391 (1997).
6. Bjørnstad, O.N., Fromentin, J.-M., Stenseth, N.C. & Gjøsæter, J. Cycles and trends in cod population. *Proc. Natl. Acad. Sci. USA* **96**, 5066-5071 (1999).